

**Compounding approach for univariate time series with nonstationary variances**

Rudi Schäfer\*

*Fakultät für Physik, Universität Duisburg-Essen, Germany*

Sonja Barkhofen†

*Applied Physics, University of Paderborn, Warburger Strasse 100, 33098 Paderborn, Germany  
and Fachbereich Physik, Philipps-Universität Marburg, Germany*

Thomas Guhr‡

*Fakultät für Physik, Universität Duisburg-Essen, Germany*

Hans-Jürgen Stöckmann§

*Fachbereich Physik, Philipps-Universität Marburg, Germany*

Ulrich Kuhl||

*Laboratoire de Physique de la Matière Condensée, CNRS UMR 7336, Université de Nice Sophia-Antipolis, F-06108 Nice, France  
and Fachbereich Physik, Philipps-Universität Marburg, Germany*

(Received 11 March 2015; revised manuscript received 12 April 2015; published 1 December 2015)

A defining feature of nonstationary systems is the time dependence of their statistical parameters. Measured time series may exhibit Gaussian statistics on short time horizons, due to the central limit theorem. The sample statistics for long time horizons, however, averages over the time-dependent variances. To model the long-term statistical behavior, we compound the local distribution with the distribution of its parameters. Here, we consider two concrete, but diverse, examples of such nonstationary systems: the turbulent air flow of a fan and a time series of foreign exchange rates. Our main focus is to empirically determine the appropriate parameter distribution for the compounding approach. To this end, we extract the relevant time scales by decomposing the time signals into windows and determine the distribution function of the thus obtained local variances.

DOI: [10.1103/PhysRevE.92.062901](https://doi.org/10.1103/PhysRevE.92.062901)

PACS number(s): 05.45.-a, 89.65.Gh, 05.40.Jc, 05.90.+m

**I. INTRODUCTION**

Due to the central limit theorem a great deal of phenomena can be described by Gaussian statistics. This also guides our perception of the risks of large deviations from an expectation value. Consequently, the occurrence of any aggravated probability of extreme events is always cause for concern and subject of intense research interest. In a large variety of systems where heavy-tailed distributions are observed, Gaussian statistics holds only locally; the parameters of the distribution are changing, either in time or in space. Thus, to describe the sample statistics for the whole system, one has to average the parametric distribution over the distribution of the (shape) parameter. This construction is known as *compounding* or *mixture* [1–3] in the mathematics and as *superstatistics* [4] in the physics literature.

An important example for parameter distribution functions is the K distribution mentioned 1978 for the first time by Jakeman and Pusey [5]. It was introduced in the context of intensity distributions, and their significance for scattering processes of a wide range of length scales was stressed. Moreover, the distribution is known to be an equilibrium solution for the population in a simple birth-death-immigration

process which was already applied in the description of eddy evolution in a turbulent medium [6]. The underlying picture of turbulence assumes that large eddies are spontaneously created and then “give birth” to generations of children eddies, which terminates when the smallest eddies die out due to viscous dissipation. In [7], Jakeman and Pusey use the K distribution for fitting data of microwave sea echo, which turned out to be highly non-Rayleigh. The K distribution is also found as a special case of a full statistical-mechanical formulation for non-Gaussian compound Markov process, developed in [8]. Field and Tough find K-distributed noise for the diffusion process in electromagnetic scattering [9,10]. Experimentally, the K distribution appeared in the contexts of irradiance fluctuations of a multipass laser beam propagating through atmospheric turbulence [11], synthetic aperture radar data [12], ultrasonic scattering from tissues [13,14], and mesoscopic systems [15]. Also in our study we will encounter the K distribution for one of the systems under consideration.

Compounded distributions can be applied to very different empirical situations: they can describe aggregated statistics for many time series, where each time series obeys stationary Gaussian statistics, the parameters of which vary only between time series. In this case, it is straightforward to estimate the parameter distribution. The situation is more difficult when we consider the statistics of single long time series with time-varying parameters. In this nonstationary case, one often makes an *ad hoc* assumption about the analytical form of the parameter distribution, and only the compounded distribution is compared to empirical findings.

\*rudi.schaefer@uni-duisburg-essen.de

†sonja.barkhofen@uni-paderborn.de

‡thomas.guhr@uni-duisburg-essen.de

§stoeckmann@physik.uni-marburg.de

||ulrich.kuhl@unice.fr

In this paper, we address the problem of determining the parameter distribution empirically for univariate nonstationary time series. Specifically, we consider the case of Gaussian statistics with time-varying variance. In this endeavor we encounter several problems: If the variance for each time point is purely random, as the compounding ansatz would suggest, we have no way of determining the variance distribution from empirical data. A prerequisite for an empirical approach to the parameter distribution is a time series which is quasistationary on short time intervals. In other words, the variance should vary only slowly compared to the time scale of fluctuations in the signal. The estimation noise for the local variances competes with the variance distribution itself. Therefore, the time interval on which quasistationarity holds should not be too short. Furthermore, we have to heed possible autocorrelations in the time series themselves since they might lead to an estimation bias for the local variances. Our aim is to test the validity of the compounding approach on two different data sets.

The paper is organized as follows: In Sec. II, we give a short summary of the compounding approach and present two recent applications where the K distribution comes into play. In Sec. III, we introduce the two systems we are going to analyze, a table-top experiment on air turbulence and the empirical time series of exchange rates between U.S. dollar and Euro. In Sec. IV, we address the problem of estimating nonstationary variances in univariate time series. Our empirical results are presented in Sec. V.

## II. COMPOUNDING ANSATZ

### A. Basics

We consider a distribution  $p(I|\alpha)$  of  $d$  random variables, ordered in the vector  $I$ . It is also a function of a parameter  $\alpha$  that determines the shape or other features of the distribution, e.g., the variance of a Gaussian. If, in a given data set, the parameter  $\alpha$  varies in an interval  $A$ , one can try to construct the distribution of  $I$  as the linear superposition

$$\langle p \rangle(I) = \int_A f(\alpha) p(I|\alpha) d\alpha \quad (1)$$

of all distributions  $p(I|\alpha)$  with  $\alpha \in A$ . Here,  $f(\alpha)$  is the weight function determining the contribution of each value of  $\alpha$  in the superposition. Since  $\alpha$  itself typically is a random variable, we assume that the function  $f(\alpha)$  is a proper distribution. In particular, it is positive semidefinite. As each  $p(I|\alpha)$  and the resulting  $\langle p \rangle(I)$  have to be normalized with respect to the random vector  $I$ , Eq. (1) implies the normalization

$$\int_A f(\alpha) d\alpha = 1. \quad (2)$$

The physics reasons for the variation of the parameter  $\alpha$  can be very different. In nonequilibrium thermodynamics,  $\alpha$  might be the locally fluctuating temperature. Although our systems are not of a thermodynamic kind, we also have in mind nonstationarities.

### B. Rayleigh distribution

In all examples discussed in this paper,  $p(I|\alpha)$  is given by a Rayleigh distribution

$$p(I|\alpha) = \frac{1}{\alpha} \exp(-I/\alpha). \quad (3)$$

Rayleigh distributions typically result from a superposition of random variables. They have been proposed more than 100 years ago by Rayleigh to describe the intensity distribution of waves in the ocean and have been studied meanwhile in many other systems elsewhere. In chaotic billiards, e. g., Berry [16] proposed to describe the wave function in a chaotic billiard by a random superposition of plane waves  $\psi_i(\vec{r}) = \exp(i\vec{k}_i\vec{r})$  entering from different directions with a fixed modulus  $k = |\vec{k}_i|$  of the wave vector

$$\psi(\vec{r}) = \frac{1}{\sqrt{N}} \sum_{i=1}^N \psi_i(\vec{r}). \quad (4)$$

As a consequence of the central limit theorem in the limit  $N \rightarrow \infty$  for closed systems Porter-Thomas distribution results for the wave-function intensities  $I = \psi^2$ . In open systems, the wave function becomes complex,  $\psi = \psi_R + i\psi_I$ , and a Rayleigh distribution is found for the average of the intensity over all positions  $\langle I \rangle_{\text{pos}} = \langle \psi_R^2 \rangle_{\text{pos}} + \langle \psi_I^2 \rangle_{\text{pos}}$ . (This is true, if the variances of the real and imaginary parts are equal, for the general case see Ref. [17].)

### C. K distribution

Let us now consider a different though related situation, where a time signal is generated by a superposition of Gaussian random variables  $\psi_i(\vec{r})$ :

$$\psi(\vec{r}, t) = \frac{1}{\sqrt{N}} \sum_{i=1}^N \psi_i(\vec{r}) e^{i\omega_i t}. \quad (5)$$

In contrast to the situation discussed above, we now assume that the number  $N$  of components is small. We then obtain for the distribution of the intensity, now averaged over the time for a fixed position, again a Rayleigh distribution

$$p(I|I_{\text{loc}}) = \frac{1}{I_{\text{loc}}} \exp(-I/I_{\text{loc}}), \quad (6)$$

where the variance  $I_{\text{loc}} = \langle I \rangle_{\text{time}}$  depends on the position. In this situation, the distribution of local variance can be calculated. It is given by a  $\chi_\nu^2$  distribution, where  $\nu$  is the number of statistically independent  $\psi_i(\vec{r})$  entering the sum in Eq. (5). Depending on the situation,  $\nu$  may be much smaller than  $N$ .

With  $f(\alpha) = \chi_\nu^2(\alpha)$  and  $\alpha = I_{\text{loc}}$  the integral (1) can be done and yields

$$\langle p \rangle(I) = \frac{\nu}{\Gamma(\frac{\nu}{2})} \left(\frac{\nu I}{2}\right)^{\frac{\nu}{4}-\frac{1}{2}} \mathcal{K}_{\frac{\nu}{2}-1} \left(2\sqrt{\frac{\nu I}{2}}\right), \quad (7)$$

where  $\mathcal{K}_\mu$  is the modified Bessel function of degree  $\mu$ . This is the K distribution introduced in the Introduction.

An example of the compounding ansatz in the aforementioned situation is given by a recent experiment [18] where we studied the propagation of microwaves through an arrangement

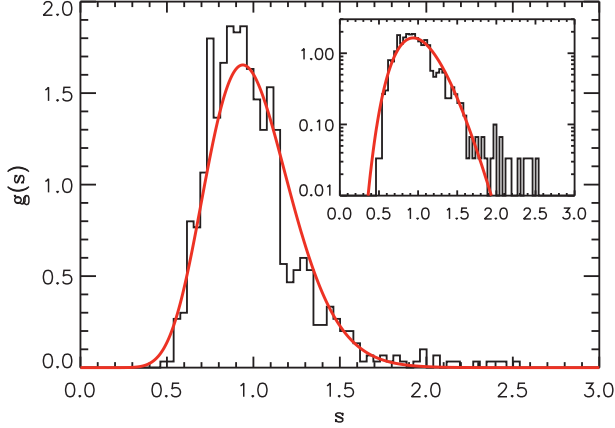


FIG. 1. (Color online) Distribution of the time-averaged intensities  $I_{\text{loc}}$  found for the 780 pixels of our measurement (for details see [18]). The inset shows the same data using a semilogarithmic scale. The solid curve is a  $\chi^2$  distribution with  $\nu = 32$  degrees of freedom.

of disordered scatterers in a cavity, corresponding to a potential landscape. From the stationary field patterns  $\psi_i(\vec{r})$  obtained in the measurement, time-dependent wave fields were generated according to Eq. (5) by superposition of  $N = 150$  patterns.

For fixed positions, indeed Rayleigh distributions were found in each time sequence  $\psi(\vec{r}, t)$  for the distribution of intensities  $I$ , with  $I_{\text{loc}}$  depending on the position. The distribution of  $I_{\text{loc}}$  turned out to be  $\chi^2_\nu$  distributed (see Fig. 1). The number  $\nu$  of degrees of freedom was related to the number of independent field components and took a value of  $\nu = 30$ .

#### D. Generalization to the multivariate case

We briefly sketch another example which stems from finance (for details see Ref. [19]). We consider a selection of  $K$  stocks with prices  $S_k(t)$ ,  $k = 1, \dots, K$ , belonging to the same market. One is interested in the distribution of the relative price changes over a fixed time interval  $\Delta t$ , also referred to as returns:

$$r_k(t) = \frac{S_k(t + \Delta t) - S_k(t)}{S_k(t)}. \quad (8)$$

For short sample windows  $T$  of a month or less, the distribution of the  $K$  component vector  $r$  can be described by a multivariate Gaussian

$$p(r|\Sigma_t) = \frac{1}{\sqrt{\det(2\pi\Sigma_t)}} \exp\left(-\frac{1}{2}r^\dagger \Sigma_t^{-1}r\right), \quad (9)$$

where  $\Sigma_t$  denotes the covariance matrix. For longer sample windows  $T$  the nonstationarity of the covariance matrix causes deviations from the Gaussian behavior. To take this into account, the fluctuating covariance matrices  $\Sigma_t$  can be approximated by an ensemble of random matrices.

In Ref. [19], a Wishart distribution was assumed for this ensemble. The ensemble average of the distribution (9) over the Wishart ensemble yields

$$\langle p \rangle(r|\Sigma, N) = \int_0^\infty \chi_N^2(z) p\left(r \left| \frac{z}{N} \Sigma \right.\right) dz, \quad (10)$$

where  $\Sigma$  is the sample-averaged covariance matrix over the entire time window  $T$ . As  $\Sigma$  is fixed, this result has the form of the compounding ansatz (1). The number  $N$  of degrees of freedom in the  $\chi_N^2$  distribution determines the variance in the distribution of the random covariance matrices. The role of the locally averaged intensity  $I_{\text{loc}}$  is now played by an effective parameter  $z$  which fully accounts for the ensemble average. Again, a K distribution follows:

$$\langle p \rangle(r|\Sigma, N) = \frac{1}{2^{\frac{N}{2}+1} \Gamma(\frac{N}{2}) \sqrt{\det(2\pi \frac{\Sigma}{N})}} \frac{\mathcal{K}_{\frac{K-N}{2}}(\sqrt{NI_\Sigma})}{(\sqrt{NI_\Sigma})^{\frac{K-N}{2}}}, \quad (11)$$

in which, roughly speaking, the bilinear form  $I_\Sigma = r^\dagger \Sigma^{-1}r$  takes the place of the intensity  $I$  in Eq. (7). This shows that K distributions may appear in very different contexts (see also the Introduction). We shall meet a further example in the next section.

### III. DATA ACQUISITION

In the last section, the compounding approach has been illustrated by two multivariate systems. For the microwave system, Rayleigh distributions were found in the generated time series for each point of the field pattern. The variances within each time series were constant and thus easily measurable, but varied from position to position. Here, the compounding corresponds to the aggregation over all positions. In the stock market example, the fluctuating covariance matrices  $\Sigma_t$  were assumed to follow a Wishart distribution. While the resulting K distribution for the intensities captures the empirical data quite well, the Wishart distribution for the covariances was merely an *ad hoc* assumption and is difficult to verify empirically. These examples have been presented to introduce the ideas, but are not part of the main topic of this paper.

We now turn to systems where only univariate time series exist, but no prior information on their possible compositions. In such a situation it is not evident whether the compounding ansatz is appropriate at all since it implies that for short times the variance is constant and changes only slowly on the scale of the typical correlation time of the fluctuations. But, if the ansatz works, and one succeeds in reducing the signal to the distribution function of its variances, then it would mean a large step towards an understanding of the origin of the signal. In the case of K distributions, e. g., it could be possible to relate the number of degrees of freedom to the hidden sources of the signal.

#### A. Turbulent air flow

The first data set is obtained by measuring the noise generated by a turbulent air flow [20]. For the turbulence generation we used a standard fan with a rotor frequency of 18.44 Hz. We restricted ourselves to standard audio technique handling frequencies up to 20 kHz and standard sampling rates of 48 kHz offering reliable quality at an attractive price. The microphone for the sound recording is a E 614 by Sennheiser with a frequency response of 40 Hz–20 kHz, a good directional characteristic and a small diameter of 20 mm. It guarantees a broadband frequency resolution and a pointlike measuring position. An external sound card with matching



FIG. 2. (Color online) Setup for the generation and measurement of the turbulent air flow. The turbulent air flow has been generated by the fan on the left hand side and recorded by the microphone in front of it. In the preliminary stage of the experiments, the sound card of the laptop has been used for data acquisition.

properties was necessary to use the full capacity of the quality of microphone and to minimize the influence of the intrinsic noise of the PC. Figure 2 shows a photograph of the used setup. A microphone has been placed in front of a fan running continuously and generating a highly turbulent air flow. The microphone records the time signal of the sound waves excited by the turbulence (for details see [20]). The analyzed time series will be discussed in detail in Sec. IV.

### B. Foreign exchange rates

The foreign exchange markets have the peculiar feature of all-day continuous trading. This is in contrast to stock markets, where the trading hours of different stock exchanges vary due to time zones, with partial overlap of different markets and very peculiar trading behavior at the beginning and the end of each trading day. Therefore, foreign exchange rates are particularly suited for the study of long time series.

We consider the time series of hourly exchange rates between Euro and U. S. dollar in the time period from January 2001 to May 2013 [21]. We denote the time series of exchange rates by  $S(t)$ . From these we calculate the time series of returns (8), i.e., the relative changes in the exchange rates on time intervals  $\Delta t$ . Since we work with hourly data, the smallest possible value for  $\Delta t$  is one hour. However, as we will see later on, a return interval of one trading day  $\Delta t = 1d$  is preferable for the variance estimation. Note that foreign exchange rates are typically modeled by a multiplicative random process, such as a geometric Brownian motion (see, e.g., [22]). Therefore, we consider the relative changes of the exchange rates instead of the exchange rates themselves. While the latter resemble, at least locally, a lognormal distribution, the returns are approximately Gaussian, conditioned on the local variance, that is.

## IV. NONSTATIONARY VARIANCES IN UNIVARIATE TIME SERIES

We consider the problem of univariate time series with time-dependent variance. More specifically, we consider time

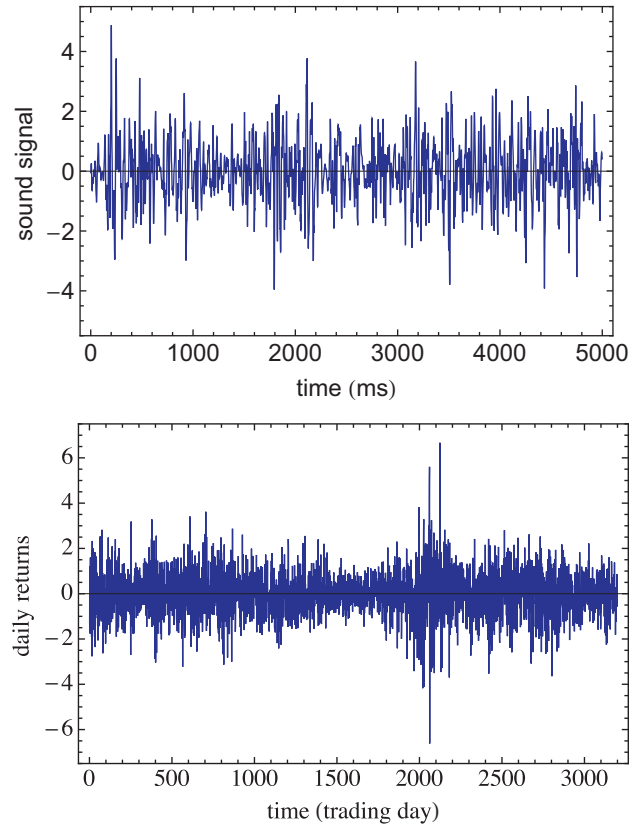


FIG. 3. (Color online) (Top) Sound signal of the ventilator measurement. (Bottom) Time series of daily returns. Both signals have been normalized to mean zero and standard deviation one. In both cases, we observe extended periods of low and high fluctuation strength.

series where the variance is changing, but exhibits a slowly decaying autocorrelation function. This point is crucial because otherwise it is not possible to make meaningful estimates of the local variances. Time series with this feature show extended periods of large fluctuations interrupted by periods with moderate or small fluctuations. This is illustrated in Fig. 3 for the two data sets we are studying in this paper. In the top plot of Fig. 3, we show the sound signal for the ventilator measurement. In the bottom plot, the time series of daily returns for the foreign exchange data is plotted. In both cases we observe the same qualitative behavior, which is well known in the finance literature as volatility clustering.

The compounding ansatz for univariate time series assumes a normal distribution on short time horizons, where the local variance is nearly stationary. However, we wish to determine the distribution of the local variances empirically since it is a critical part in the compounding ansatz. If the variances were fluctuating without a noticeable time-lagged correlation, this would not be feasible. Still, we need to establish the right time horizon on which to estimate the local variances. Reference [23] introduced a method to locally normalize time series with autocorrelated variances. To this end, a local average was subtracted from the data and the result was divided by a local standard deviation. In this spirit, we determine the time horizon on which this local normalization yields normal distributed values and analyze the corresponding local variances.

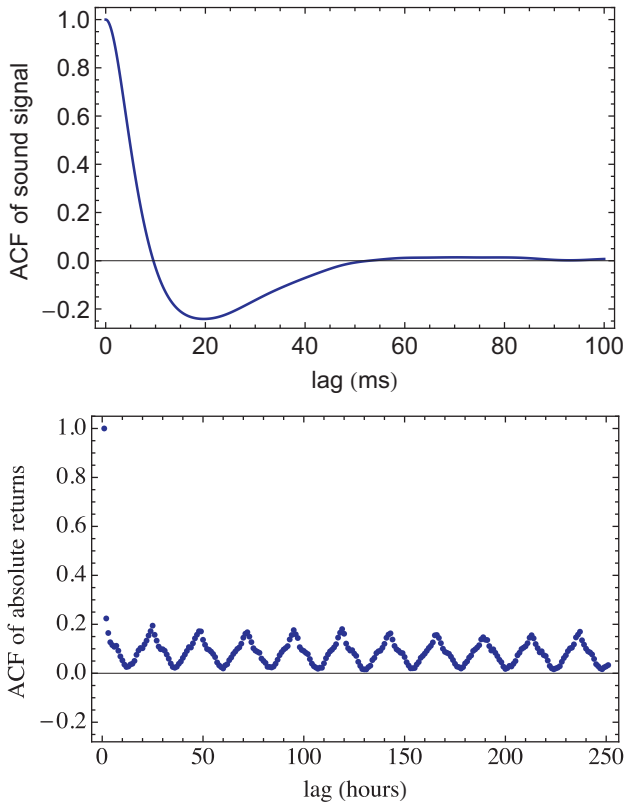


FIG. 4. (Color online) (Top) Autocorrelation function of the measured sound signal. (Bottom) Autocorrelation function of the absolute values of hourly returns.

Another aspect we need to take into account is a possible bias in the variance estimation which occurs for correlated events. In Fig. 4, we show the autocorrelation function (ACF) of the measured sound signal, as well as the autocorrelation function of the absolute value of hourly returns. Both plots hint at possible problems for the variance estimation. Due to the high sampling frequency, the sound signal is highly correlated. In other words, the sampling time scale is much shorter than the time scale on which the turbulent air flow changes. After 2500 data points, or about 52 ms, the autocorrelation function has decayed to zero. Consequently, we consider only every 2500th data point for our local variance estimation. To improve statistics, we repeat the variance estimation starting with an offset of 1 to 2499. The results are presented in the following section.

In the case of the foreign exchange data we are confronted with a different problem. The consecutive hourly returns are not correlated. While local trends may always exist, it is unpredictable when a positive trend switches to a negative one, and *vice versa* (see Ref. [24]). However, the autocorrelation of the absolute values shows a rich structure which is due to characteristic intraday variability. This would lead to a biased variance estimation and, consequently, to a distortion of the variance distribution. Therefore, we consider returns between consecutive trading days at the same hour of the day. Put differently, we consider  $\Delta t = 1 \text{ d}$  for the returns and get 24 different time series, one for each hour of the day as starting point.

V. EMPIRICAL RESULTS

We first discuss the results for the turbulent air flow. As described in the previous section, we sliced the single measurement time series into 2500 time series with lower sampling rate, taking only every 2500th measurement point. This is necessary to avoid a bias in the estimation of the local variances. Before proceeding, each of these time series is globally normalized to mean zero and standard deviation one. Figure 5 shows the empirical results for the distribution of local variances and the compounded distribution. The local variances are rather well described by a  $\chi^2$  distribution with  $N$  degrees of freedom. We find  $N = 10$  to provide the best fit to the data. The distribution of the empirical sound amplitudes is well described by a K distribution with the same  $N$  which fits the variance distribution. Hence, we arrive at a consistent picture, which supports our compounding ansatz for this measurement.

The results for the daily returns of EUR-USD foreign exchange rates are shown in Fig. 6. As outlined in Sec. IV, we calculated the daily returns as the relative changes of the exchange rate between consecutive trading days with respect to the same hour of each day. This procedure yields 24 time series of daily returns. We normalize each time series to mean zero and standard deviation one. This allows us to produce a single aggregated statistics. In the top plot of Fig. 6 we

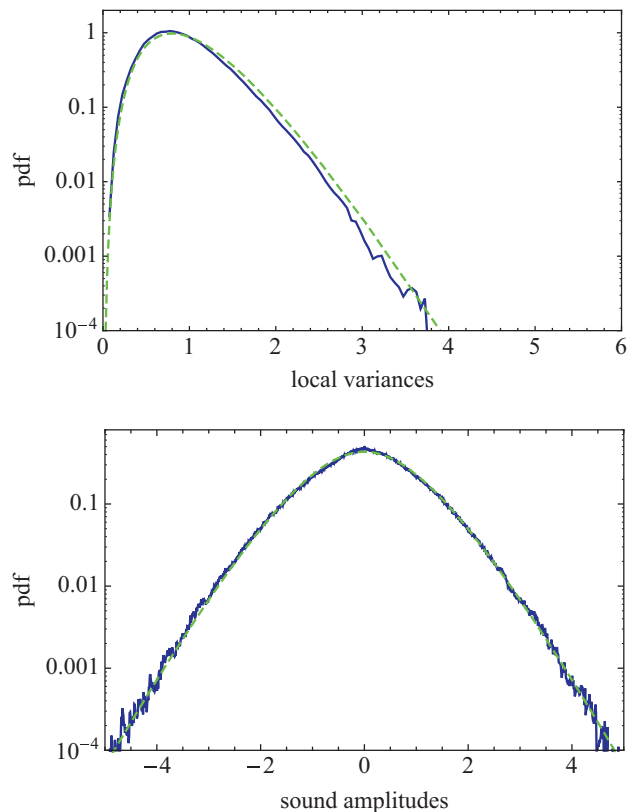


FIG. 5. (Color online) Results for the turbulent air flow. (Top) Distribution of variances, compared to a  $\chi^2$  distribution with  $N = 10$  degrees of freedom (dashed green line). (Bottom) Distribution of the sound amplitudes, compared to the K distribution with parameter  $N = 10$  (dashed green line).

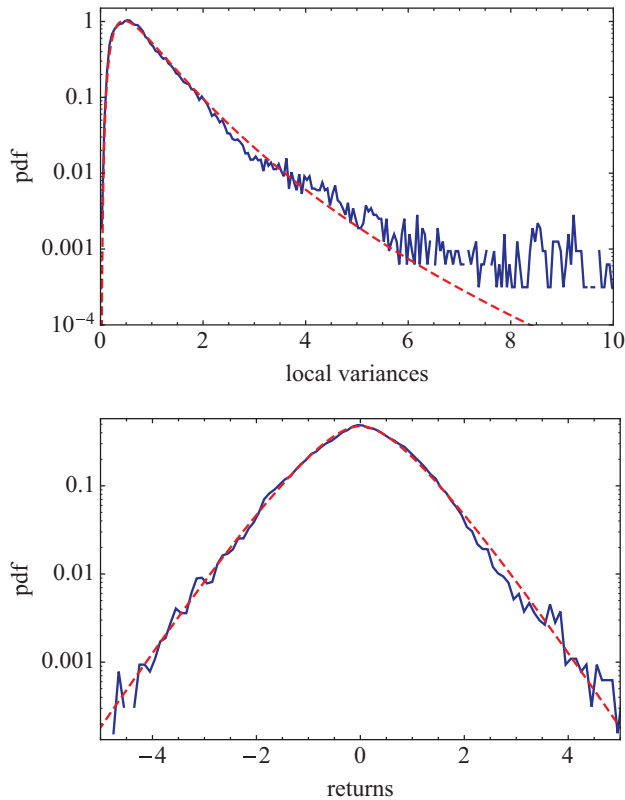


FIG. 6. (Color online) Results for daily returns of foreign exchange rates EUR-USD. (Top) Distribution of variances, compared to a lognormal distribution (dashed red line). (Bottom) Distribution of the daily returns, compared to a lognormal compounded distribution (dashed red line).

show the histogram of local variances, i.e., the variances estimated on 13-day intervals. The empirical variances follow a lognormal distribution over almost three orders of magnitude, with only some deviations in the tail. This is in accordance with the finance literature, where normal-lognormal mixtures have first been suggested to describe commodity prices [25], and later stock prices [26] and foreign exchange rates [27]. According to [28], the occurrence of the lognormal distribution points to an information cascade reminiscent of the energy cascade in turbulence. The histogram of the daily returns is shown in the bottom plot of Fig. 6. The empirical result agrees rather well with the normal-lognormal compounded distribution. It is important to note, however, that we only achieve this consistent picture of variance and compounded return distribution because we have taken into account all the pitfalls of variance estimation, which we described in Sec. IV.

## VI. CONCLUSIONS

In a large variety of systems we encounter time series that exhibit Gaussian statistics locally, where the variances are nonstationary. In such a setting, a compounding approach can be used to describe the sample statistics on large time scales. For demonstration we applied the compounding approach to two very different systems, a ventilator setup generating turbulent air flow and foreign exchange rates. Both systems

are characterized by univariate time series with nonstationary variances. Our main objective was to empirically determine the distribution of variances and thus arrive at a consistent picture. The estimation of variances from a single, nonstationary time series presents several pitfalls, which have to be taken into account carefully. First of all, we have to avoid serial correlations in the signal itself. These might otherwise lead to an estimation bias. For the sound measurement, we had to reduce the sampling rate of the data to achieve this. The foreign exchange data presented another obstacle for variance estimation: We observed a characteristic intraday variability which had to be taken into account. Last but not least, it is a prerequisite that the nonstationary variances are not purely stochastic, but exhibit a slowly decaying autocorrelation. Otherwise, we would not be able to determine a reasonable variance distribution for the compounding ansatz. When we take all these aspects into account, we arrive at the correct variance distribution. In good approximation we found a  $\chi^2$  distribution in the case of ventilator turbulence, which leads to a K distribution for the compounded statistics. For the foreign exchange returns we observe lognormal distributed variances; and the normal-lognormal compounded distribution fit the return histogram well.

In cases where the intensities are K distributed with  $\nu$  degrees of freedoms, it seems worthwhile to look whether it is possible to trace back the time signal to  $\nu$  independent sources. For the turbulent flow discussed in this paper, these sources might be the dominant vortex structures. Controlled experiments are needed to check this conjecture. In favorable cases the variance distributions of the time signal might even be used to monitor the underlying structures. Lognormal distributed variances, as they are found in the time series extracted from the stock market, suggest an information cascade reminiscent of the energy cascade in turbulence [28].

Why is it so important to get an empirical handle on the variance distributions themselves? They reflect the system behavior and might not even be stationary. Here, we restricted ourselves to two examples where the variance distribution is well described by a simple  $\chi^2$  or a simple lognormal distribution, since we aimed to explore the pitfalls of determining the variance distribution.

However, things become even more interesting when the variance distribution also changes in time. Our table-top experiment on turbulent air flow corresponded to a well-controlled setting where the characteristics of the generated turbulence are rather stable. In contrast, the turbulence observed in a wind park, for instance, is not as steady, but subject to changing weather conditions on larger scales. Similarly, distinct market states have recently been observed for stock markets [29], implying a richer structure of the covariance matrix ensemble than a simple Wishart distribution [30]. Our present study is a first step towards an empirical assessment of these and similar highly nonstationary systems.

## ACKNOWLEDGMENT

The sound measurements have been supported by the Deutsche Forschungsgemeinschaft via the Forschergruppe 760 “Scattering Systems with Complex Dynamics.”

- [1] S. D. Dubey, Compound gamma, beta and F distributions, *Metrika* **16**, 27 (1970).
- [2] O. Barndorff-Nielsen, J. Kent, and M. Sørensen, Normal variance-mean mixtures and z distributions, *Int. Stat. Rev.* **50**, 145 (1982).
- [3] A. P. Doulgeris and T. Eltoft, Scale mixture of Gaussian modelling of polarimetric SAR data, *EURASIP J. Adv. Sig. Pr.* **2010**, 874592 (2010).
- [4] D. Beck and E. G. D. Cohen, Superstatistics, *Phys. A (Amsterdam)* **322**, 267 (2003).
- [5] E. Jakeman and P. N. Pusey, Significance of K Distributions in Scattering Experiments, *Phys. Rev. Lett.* **40**, 546 (1978).
- [6] E. Jakeman, On the statistics of K-distributed noise, *J. Phys. A: Math. Gen.* **13**, 31 (1980).
- [7] E. Jakeman and P. N. Pusey, A model for non-Rayleigh sea echo, *IEEE Trans. Antennas Propag.* **24**, 806 (1976).
- [8] E. Jakeman and R. J. A. Tough, Non-Gaussian models for the statistics of scattered waves, *Adv. Phys.* **37**, 471 (1988).
- [9] T. R. Field and R. J. A. Tough, Diffusion processes in electromagnetic scattering generating K-distributed noise, *Proc. R. Soc. London, Ser. A* **459**, 2169 (2003).
- [10] T. R. Field and R. J. A. Tough, Stochastic dynamics of the scattering amplitude generating K-distributed noise, *J. Math. Phys.* **44**, 5212 (2003).
- [11] A. K. Majumdar and H. Gamo, Statistical measurements of irradiance fluctuations of a multipass laser beam propagated through laboratory-simulated atmospheric turbulence, *Appl. Opt.* **21**, 2229 (1982).
- [12] J. S. Lee, D. L. Schuler, R. H. Lang, and K. J. Ranson, K-distribution for multi-look processed polarimetric SAR imagery, in *Geoscience and Remote Sensing Symposium, 1994. IGARSS'94. Surface and Atmospheric Remote Sensing: Technologies, Data Analysis and Interpretation* (IEEE, New York, 1994), Vol. 4, pp. 2179–2181.
- [13] P. M. Shankar, A model for ultrasonic scattering from tissues based on the K distribution, *Phys. Med. Biol.* **40**, 1633 (1995).
- [14] L. Weng, J. M. Reid, P. M. Shankar, and K. Soetanto, Ultrasound speckle analysis based on the K distribution, *J. Acoust. Soc. Am.* **89**, 2992 (1991).
- [15] L. R. Arnaut, Sampling distributions of random electromagnetic fields in mesoscopic or dynamical systems, *Phys. Rev. E* **80**, 036601 (2009).
- [16] M. V. Berry, Regular and irregular semiclassical wavefunctions, *J. Phys. A: Math. Gen.* **10**, 2083 (1977).
- [17] R. Pnini and B. Shapiro, Intensity fluctuations in closed and open systems, *Phys. Rev. E* **54**, R1032 (1996).
- [18] R. Höhmann, U. Kuhl, H.-J. Stöckmann, L. Kaplan, and E. J. Heller, Freak Waves in the Linear Regime: A Microwave Study, *Phys. Rev. Lett.* **104**, 093901 (2010).
- [19] Thilo A. Schmitt, Desislava Chetalova, Rudi Schäfer, and Thomas Guhr, Non-stationarity in financial time series: Generic features and tail behavior, *Europhys. Lett.* **103**, 58003 (2013).
- [20] S. Barkhofen, Microwave Measurements on n-Disk Systems and Investigation of Branching in correlated Potentials and turbulent Flows, Ph.D. thesis, Philipps-Universität Marburg, 2013.
- [21] The empirical data were obtained from [www.fxhistoricaldata.com](http://www.fxhistoricaldata.com)
- [22] Nahum Biger and John Hull, The valuation of currency options, *Finan. Manage.* **12**, 24 (1983).
- [23] R. Schäfer and T. Guhr, Local normalization: Uncovering correlations in non-stationary financial time series, *Phys. A (Amsterdam)* **389**, 3856 (2010).
- [24] Tobias Preis, Johannes J Schneider, and H. Eugene Stanley, Switching processes in financial markets, *Proc. Natl. Acad. Sci. USA* **108**, 7674 (2011).
- [25] Peter K. Clark, A subordinated stochastic process model with finite variance for speculative prices, *Econometrica: J. Econometric Soc.* **41**, 135 (1973).
- [26] George E. Tauchen and Mark Pitts, The price variability-volume relationship on speculative markets, *Econometrica: J. Econometric Soc.* **51**, 485 (1983).
- [27] David A. Hsieh, Modeling heteroscedasticity in daily foreign-exchange rates, *J. Bus. Econ. Stat.* **7**, 307 (1989).
- [28] Shoaleh Ghashghaie, Wolfgang Breymann, Joachim Peinke, Peter Talkner, and Yadollah Dodge, Turbulent cascades in foreign exchange markets, *Nature (London)* **381**, 767 (1996).
- [29] Michael C. Münnix, Takashi Shimada, Rudi Schäfer, Francois Leyvraz, Thomas H. Seligman, Thomas Guhr, and H. Eugene Stanley, Identifying states of a financial market, *Sci. Rep.* **2**, 644 (2012).
- [30] Desislava Chetalova, Rudi Schäfer, and Thomas Guhr, Zooming into market states, *J. Stat. Mech.* (2015) P01029.